

SOLVING THE MILD-SLOPE AND HELMHOLTZ EQUATIONS USING THE VIRTUAL ELEMENT METHOD (VEM), DEALING WITH HIGH ORDER ROBIN BOUNDARY CONDITION

R. Dupont^{1,2} and M. Dauphin³, R. Mottier^{4,5,6}

July 17, 2024

¹ GEOSCIENCES-M, Univ Montpellier, CNRS, Montpellier, France.

² IMAG, Univ Montpellier, CNRS, Montpellier, France.

³ Scuola Superiore Meridionale, Napoli, Italy.

⁴ École nationale des ponts et chaussées, France.

⁵ Commissariat à l'énergie atomique et aux énergies alternatives, France.

⁶ Institut national de recherche en sciences et technologies du numérique,
France.

*Corresponding authors. E-mail(s): ronan.dupont@umontpellier.fr;
mathias.dauphin-ssm@unina.it; romain.mottier@outlook.com.

Abstract

The numerical solution of the Mild-slope equation (MSE) is crucial in various fields, including coastal engineering, oceanography, and offshore structure design. In this article, we present a novel approach utilizing the Virtual Element Method (VEM) for the numerical solution of the MSE. The VEM offers significant advantages over traditional finite element methods, particularly in handling complex geometries and irregular meshes. We first look at the implementation and validation of the model in the presence of Robin boundary conditions. We then apply the results to the calculation of eigenmodes for the port of Cherbourg.

Keywords. Mild-slope equation, Helmholtz equation, Virtual Element Method, computational fluid dynamics, validation, Finite Element Methods, Numerical Analysis, Complex Geometries, Irregular Meshes, Robin Boundary Condition, Coastal Engineering.

Contents

1	Introduction	3
2	Problem (section qui va pas ici)	3
3	VEM	5
3.1	Dofs	5
3.2	pb	5
3.3	Robin Boundary Condition	9
4	Numerical Validation	12
5	Numerical Application	13
5.1	Sensibilité de la pente, helmoltz vs Berkhoff	13
5.2	Application claquée - Résultats avec différents k	13
5.3	Sensibilité du coefficient de réflexion	13
5.4	Appli montrant intérêt Robin	14
6	Conclusion and Discussion	16
7	Declarations	17
7.1	Availability of data and material	17
7.2	Conflict of interest	17
7.3	Acknowledgements	17
A	Roro pue	18

1 Introduction

Nowadays, coastal modeling has become a major challenge in the face of climate change. Coastal-related topics have become very numerous, including ocean modeling (large-scale), port modeling and numerous other topics such as morphodynamics. In this study, we are particularly interested in port modeling through the equation models developed by Helmholtz (1868) and Berkhoff (1972). These two equation models can be used in coastal modeling to calculate wave agitation inside a harbor. The Helmholtz (1868) equation is a very classical equation, which can be used in various fields such as electromagnetics or acoustics. In our study, it is used for flat sea bottoms, while the Berkhoff (1972) equation, also known as the Mild-Slope equation, is used for variable bottoms with a maximum slope of 1/3 (Booij 1983). In this study, we have chosen to solve these equations using the virtual element method (Beirão da Veiga et al. 2014) ~~MATHIAS, tu peux ajouter qqrs autres refs importantes stp.~~. This method has the advantage of i) being a high-order finite element method, which enables wave phenomena to be accurately captured, where simple finite elements have difficulty capturing them ~~RORO, tu peux ajouter des références pour ce que tu disais, que sur des méthodes FEM simple, même en raffinement, on arrivait pas à capturer tous les phénomènes ondulatoires.~~, ii) handle polyhedral meshes as well as non-conforming meshes, enabling simple refinement in certain areas. Although a few studies have already dealt with the Helmholtz (1868) problem in virtual elements (Perugia et al. 2016; Mascotto et al. 2019), none of them has had any concrete application in the coastal sector. In this study, we will first express the modeling of the problem. Next, we will explain the virtual element strategy for approximating this problem. Finally, we'll look at a particular boundary condition, the Robin condition. After validating our model, we will apply it to the calculation of eigenvalues for the port of Cherbourg.

2 Problem (section qui va pas ici)

We consider $\zeta(\mathbf{x}, t) = \Re \{ \eta(x, y) e^{-i\omega t} \}$

$$u = u_i + u_r$$

with u_i the **incident wave** and u_r the **reflected wave**. We have,

$$u_i(\mathbf{x}, t) = a_i(\mathbf{x})e^{-i\sigma t} \quad \text{and} \quad u_r(\mathbf{x}, t) = a_r(\mathbf{x})e^{-i\sigma t}$$

with $\sigma = 2\pi/T_0$, the **angular frequency** and

$$a_i(\mathbf{x}) = a_{\max} e^{-i\mathbf{k}\mathbf{x}} \quad \text{with} \quad \mathbf{k} = k(\cos(\theta), \sin(\theta))$$

with θ the **incident wave angle**, a_{\max} the **maximum wave amplitude**. a_r satisfies the following Berkhoff equation :

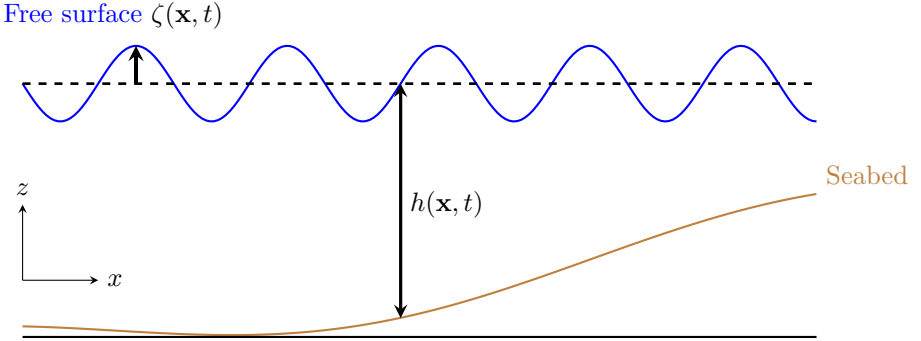


Figure 1: Sketch of a free surface elevation ζ in the (x, z) -plane.

$$\begin{cases} \nabla(C_p C_g \nabla a) + k^2 C_p C_g a = 0 & , \quad \text{in } \Omega , \\ a = -a_i & , \quad \text{on } \Gamma_D , \\ \frac{\partial a}{\partial n} + i k a = 0 & , \quad \text{on } \Gamma_{Inf}. \end{cases} \quad (1)$$

Assuming constant depth within the port and $C_g = C_p/2$ (as in shallow water) and noting that $C_p = \sigma/k = Cte$, equation (1) can be simplified to yield the following Helmholtz equation:

$$\begin{cases} \Delta a + k^2 a = 0 & , \quad \text{in } \Omega , \\ a = -a_i & , \quad \text{on } \Gamma_D , \\ \frac{\partial a}{\partial n} + i k a = 0 & , \quad \text{on } \Gamma_{Inf}. \end{cases} \quad (2)$$

Nous considérons l'hypothèse suivante:

FAUX, à mieux redire:

$$\int_E C_p C_g = Cte \quad \text{and} \quad \int_E k^2 C_p C_g = Cte \quad (3)$$

3 VEM

3.1 Dofs

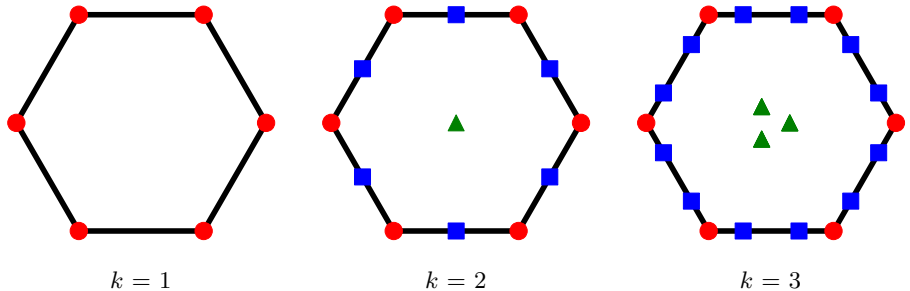


Figure 2: 2D element with ● : Summits dofs, ■ : Edges dofs, ▲ : Inner dofs.

3.2 pb

Nous considérons les problèmes suivant:

$$\begin{cases} \nabla(C_p C_g \nabla a) + k^2 C_p C_g a = 0 & , \quad \text{in } \Omega, \\ a = -a_i & , \quad \text{on } \Gamma_D, \\ \frac{\partial a}{\partial n} + i k a = 0 & , \quad \text{on } \Gamma_{Inf}. \end{cases} \quad (4)$$

On considère la formulation variationnelle:

$$\begin{cases} \text{find } u \in V = H_0^1(\Omega) \text{ such that} \\ a(u, v) = 0 \quad \forall v \in V, \end{cases} \quad (5)$$

where

$$a(u, v) = \int_{\Omega} \nabla(C_p C_g \nabla u) v + \int_{\Omega} k^2 C_p C_g u v . \quad (6)$$

We will build a discrete problem in following form:

$$\begin{cases} \text{find } u_h \in V_h \subset V \text{ such that} \\ a(u_h, v_h) = 0 \quad \forall v \in V, \end{cases} \quad (7)$$

where

- $V_h \subset V$ is a finite dimensional space;
- $a_h(\cdot, \cdot) : V_h \times V_h \rightarrow \mathbb{R}$ is a discrete bilinear form approximating the continuous form $a(\cdot, \cdot)$;

and,

$$\begin{aligned}
a_h(u_h, v_h) &= \sum_{E \in \Omega_h} \left[\int_E \nabla(\textcolor{orange}{C}_p \textcolor{orange}{C}_g \nabla u_h v_h) + \int_E k^2 \textcolor{orange}{C}_p \textcolor{orange}{C}_g u_h v_h \right], \\
&\underset{\substack{1/E \int_E \textcolor{orange}{C}_p \textcolor{orange}{C}_g = \mathcal{A}_E \\ 1/E \int_E k^2 \textcolor{orange}{C}_p \textcolor{orange}{C}_g = \mathcal{B}_E}}{\approx} \sum_{E \in \Omega_h} \left[\mathcal{A}_E \int_E (\Delta u_h v_h) + \mathcal{B}_E \int_E u_h v_h \right], \\
&\underset{\substack{green \\ \partial u / \partial n = -ik u}}{=} \sum_{E \in \Omega_h} \left[-\mathcal{A}_E \int_E \nabla u_h \nabla v_h + \mathcal{B}_E \int_E u_h v_h - \mathbf{1}_{\Gamma_{\text{Inf}} \subset E} i \mathcal{A}_E \int_{\Gamma_{\text{Inf}}} k u_h v_h \right]. \tag{8}
\end{aligned}$$

with $\mathbf{1}_{\Gamma_{\text{Inf}} \subset E}$ the indicator function and $u = u + u_D$ and u_D is the lifting of $-a_i$.

Nous considérons les problèmes suivant:

$$\begin{cases} \Delta a + k^2 a = 0 & , \quad \text{in } \Omega , \\ a = -a_i & , \quad \text{on } \Gamma_D , \\ \frac{\partial a}{\partial n} + i k a = 0 & , \quad \text{on } \Gamma_{Inf} . \end{cases} \quad (9)$$

On considère la formulation variationnelle:

$$\begin{cases} \text{find } u \in V = H_0^1(\Omega) \text{ such that} \\ a(u, v) = 0 \quad \forall v \in V , \end{cases} \quad (10)$$

where

$$\begin{aligned} a(u, v) &= \int_{\Omega} \Delta u v + k^2 \int_{\Omega} u v + k^2 \int_{\Gamma_{Inf}} \frac{\partial u}{\partial n} v \\ &= \int_{\Omega} \Delta u v + k^2 \int_{\Omega} u v - ik \int_{\Gamma_{Inf}} u v . \end{aligned} \quad (11)$$

We will build a discrete problem in following form:

$$\begin{cases} \text{find } u_h \in V_h \subset V \text{ such that} \\ a(u_h, v_h) = 0 \quad \forall v \in V , \end{cases} \quad (12)$$

where

- $V_h \subset V$ is a finite dimensional space;
- $a_h(\cdot, \cdot) : V_h \times V_h \rightarrow \mathbb{R}$ is a discrete bilinear form approximating the continuous form $a(\cdot, \cdot)$;

and,

$$\begin{aligned} a_h(u_h, v_h) &= \sum_{E \in \Omega_h} \left[\int_E \Delta u_h v_h + \int_E k^2 u_h v_h \right] , \\ &\stackrel{\text{green}}{=} \sum_{\substack{E \in \Omega_h \\ \partial u / \partial n = -iku}} \left[- \int_E \nabla u_h \nabla v_h + \int_E u_h v_h - \mathbf{1}_{\Gamma_{Inf} \subset E} i \int_{\Gamma_{Inf}} k u_h v_h \right] . \end{aligned} \quad (13)$$

with $\mathbf{1}_{\Gamma_{Inf} \subset E}$ the indicator function and $u = u + u_D$ and u_D is the lifting of $-a_i$.

Let Ω_h be a simple polygonal mesh on Ω . This can be any decomposition of Ω in non overlapping polygons E with straight faces. The space V_h will be defined element-wise, by introducing

- local spaces $V_{h|E}$;
- the associated local degrees of freedom.

For all $E \in \Omega_h$:

$$V_{h|E} = \left\{ v_h \in H_0^1(\Omega) \cap C^0(\partial E) : v_h|_{\partial E} \in \mathbb{P}_k(E), \Delta v_h \in \mathbb{P}_k(E) \right. \\ \left. (\Pi_k^\nabla v_h - v_h, p)_{0,E} = 0, \forall p \in \mathbb{P}_k(E)/\mathbb{P}_{k-2}(E) \right\} \quad (14)$$

where $\mathbb{P}_k(E)/\mathbb{P}_{k-2}(E)$ is the subspace of $\mathbb{P}_k(E)$ of the polynomials that are orthogonal in the sense of L^2 to $\mathbb{P}_{k-2}(E)$, or, alternatively, the polynomials of degree $k-1$ and k .

- the functions $V_{h|E}$ are continuous (and known) on ∂E ;
- the functions $V_{h|E}$ are unknown on E !
-

1. Mesh Decomposition: We consider a polytopal decomposition $\{T_h\}_h$ of the domain Ω which is regular—that is, there exists $\rho \in (0, 1)$, independent of h , such that every element $E \in T_h$ is star-shaped with respect to a ball of radius $\geq \rho h_E$, with h_E the diameter of E .

2. Local Projections: We denote by $\Pi_k^{\nabla, E} : H^1(E) \rightarrow \mathbb{P}_k(E)$ and $\Pi_k^{0, E} : L^2(E) \rightarrow \mathbb{P}_k(E)$ the usual lo elliptic projection and local L^2 -projection respectively onto the space of polynomials of degree a most k .

3. Virtual Space: We define the local virtual space by

$$V_h^E = \left\{ v_h \in H_0^1(\Omega) \cap C^0(\partial E) : v_h|_{\partial E} \in \mathbb{P}_k(E), \Delta v_h \in \mathbb{P}_k(E) \right. \\ \left. (\Pi_k^\nabla v_h - v_h, p)_{0, E} = 0, \forall p \in \mathbb{P}_k(E)/\mathbb{P}_{k-2}(E) \right\}$$

where $\mathbb{P}_k(E)/\mathbb{P}_{k-2}(E)$ is the subspace of $\mathbb{P}_k(E)$ of the polynomials that are orthogonal in the sense of L^2 to $\mathbb{P}_{k-2}(E)$, or, alternatively, the polynomials of degree $k-1$ and k .

3. DDL

4. Base:

$$m_{\alpha_1, \alpha_2} = \left(\frac{x - x_D}{h_D} \right)^{\alpha_1} \cdot \left(\frac{y - y_D}{h_D} \right)^{\alpha_2}$$

Soit $V = \{v \in H^1(\Omega), v|_{\Gamma_D} = 0\}$.

$$\int_{\Omega} \Delta u v + \int_{\Omega} k^2 u v = 0, \quad \forall v \in V.$$

En appliquant la formule de Green, on a :

$$-\int_{\Omega} \nabla u \nabla v + \int_{\Gamma_{Inf}} \frac{\partial u}{\partial n} v + k^2 \int_{\Omega} u v = 0, \quad \forall v \in V.$$

$$-\int_{\Omega} \nabla u \nabla v - ik \int_{\Gamma_{Inf}} u v + k^2 \int_{\Omega} u v = 0, \quad \forall v \in V.$$

3.3 Robin Boundary Condition

Nous allons construire la matrice $B = (\int_{\partial\Omega} \alpha(\Phi_j(x, y), \Phi_i(x, y))_{i,j})$ en parcourant les éléments frontières du bord. Ces éléments sont des segments joignant 2 points consécutifs du bord. La fonction de base Φ_i attachée au sommet i du bord, restreinte à l'élément de bord est une fonction \mathbb{P}_k du bord.

Les éléments du bord sont de longueur $\lambda(e)$. Pour un élément de référence de la forme $[\xi_0, \xi_0 + \lambda]$ entre deux points V_0 et V_1 .

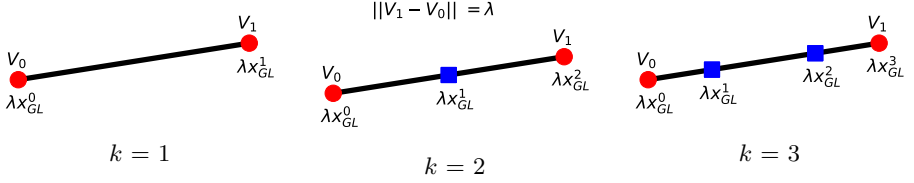


Figure 3: 1D element $[\xi_0, \xi_0 + \lambda]$ representation with ● : Summits dofs, ■ : Edges dofs.

La matrice élémentaire associée à ce terme de Robin est de la forme

$$elb = \left(\int_0^\lambda \alpha_*(\xi_0 + \xi) \varphi_j(\xi) \varphi_i(\xi) d\xi \right)_{1 \leq i, j \leq k+1}, \quad (15)$$

avec $\alpha_*(\xi_0 + \xi) = \alpha(V_0|_x + \xi t_x, V_0|_y + \xi t_y)$ et \vec{t} est le vecteur unitaire orienté de V_0 à V_1 . Pour $i, j \in \llbracket 0, k \rrbracket$:

$$\varphi_i(\lambda x_{GL}^j) = \delta_j^i,$$

avec x_{GL}^j le $j - i$ eme point de quadrature de Gauss-Lobatto sur $[0, 1]$. On trouve les φ_i aisément avec les polynômes de Lagrange comme suivant:

$$\begin{aligned} \varphi_i(\xi) &= \sum_{j=0}^k \delta_j^i \left(\prod_{l=0, l \neq j}^k \frac{\xi - \lambda x_{GL}^l}{\lambda x_{GL}^j - \lambda x_{GL}^l} \right) \\ &= \frac{1}{\lambda^k} \prod_{l=0, l \neq i}^k \frac{\xi - \lambda x_{GL}^l}{x_{GL}^i - x_{GL}^l} \end{aligned}$$

Remark:

$$\begin{aligned}
& \left(\int_0^\lambda \alpha_*(\xi_0 + \xi) \varphi_j(\xi) \varphi_i(\xi) d\xi \right)_{0 \leq i, j \leq k} \\
&=_{\alpha_* = \alpha = cte} \left(\frac{\alpha}{\lambda^{2k}} \int_0^\lambda \left[\prod_{l=0, l \neq i}^k \frac{\xi - \lambda x_{\text{GL}}^l}{x_{\text{GL}}^i - x_{\text{GL}}^l} \prod_{l=0, l \neq i}^k \frac{\xi - \lambda x_{\text{GL}}^l}{x_{\text{GL}}^j - x_{\text{GL}}^l} \right] d\xi \right)_{0 \leq i, j \leq k} \\
&=_{\substack{\xi = \lambda \xi' \\ d\xi = \lambda d\xi'}} \left(\frac{\alpha}{\lambda^{2k}} \int_0^1 \left[\prod_{l=0, l \neq i}^k \frac{\lambda \xi' - \lambda x_{\text{GL}}^l}{x_{\text{GL}}^i - x_{\text{GL}}^l} \prod_{l=0, l \neq i}^k \frac{\lambda \xi' - \lambda x_{\text{GL}}^l}{x_{\text{GL}}^j - x_{\text{GL}}^l} \right] \lambda d\xi' \right)_{0 \leq i, j \leq k} \\
&= \left(\frac{\alpha}{\lambda^{2k}} \int_0^1 \left[\prod_{l=0, l \neq i}^k \lambda \frac{\xi' - x_{\text{GL}}^l}{x_{\text{GL}}^i - x_{\text{GL}}^l} \prod_{l=0, l \neq i}^k \lambda \frac{\xi' - x_{\text{GL}}^l}{x_{\text{GL}}^j - x_{\text{GL}}^l} \right] \lambda d\xi' \right)_{0 \leq i, j \leq k} \\
&= \left(\alpha \lambda \int_0^1 \left[\prod_{l=0, l \neq i}^k \frac{\xi' - x_{\text{GL}}^l}{x_{\text{GL}}^i - x_{\text{GL}}^l} \prod_{l=0, l \neq i}^k \frac{\xi' - x_{\text{GL}}^l}{x_{\text{GL}}^j - x_{\text{GL}}^l} \right] d\xi \right)_{0 \leq i, j \leq k} \\
&= \alpha \lambda \left(\int_0^1 \tilde{\varphi}_j(\xi) \tilde{\varphi}_i(\xi) d\xi \right)_{0 \leq i, j \leq k} \tag{16}
\end{aligned}$$

with $\tilde{\varphi}_i$ the polynomials for a unit element $[\xi_0, \xi_0 + 1]$

Et par exemple pour $k = 1$, $\varphi_1(\xi) = \frac{\lambda - \xi}{\lambda}$, $\varphi_2(\xi) = \frac{\xi}{\lambda}$.

Pour le cas particulier où $\alpha = cte$, l'intégrale (15) revient à intégrer un polynôme de degrés $2k$. En évaluant celle-ci par $k + 2$ points de GL (car exacte à $2n - 3$), on obtient l'intégrale exacte.

Nous allons construire également le second membre SMB qui provient des termes de bord inhomogènes:

$$SMB_i = \int_{\partial\Omega} b(x, y) \Phi_i(x, y).$$

Ce terme est non trivialement nul si le sommet i appartient à $\partial\Omega = \Gamma_b \cup \Gamma_t \cup \Gamma_l \cup \Gamma_r$. Pour un élément de référence de la forme $[\xi_0, \xi_0 + \delta]$, le vecteur élémentaire associé à ce terme inhomogène est de la forme

$$vecb = \left(\int_0^\lambda b_*(\xi_0 + \xi) \varphi_i(\xi) d\xi \right)_{1 \leq i \leq k+1},$$

avec $\varphi_1(\xi) = \frac{\delta - \xi}{\delta}$, $\varphi_2(\xi) = \frac{\xi}{\delta}$ et $\beta_*(\xi_0 + \xi)$ coïncide avec $\beta_*(\xi_0 + \xi) = \beta(V_0|_x + \xi t_x, V_0|_y + \xi t_y)$ et \vec{t} est le vecteur unitaire orienté de V_0 à V_1 . Également, cette intégrale pourra être intégrée par GL.

4 Numerical Validation

We consider,

$$\begin{cases} \Delta u + k^2 u = f(x, y) & , \quad \text{in } \Omega, \\ u = u_{\text{exact}} & , \quad \text{on } \Gamma_2 \cup \Gamma_3 \cup \Gamma_4, \\ \frac{\partial u}{\partial n} + i k u = g(x, y) & , \quad \text{on } \Gamma_1, \end{cases} \quad \begin{array}{c} \Gamma_3 \\ \Omega \\ \Gamma_2 \\ \Gamma_1 \end{array} \quad (17)$$

with,

$$\begin{aligned} u_{\text{exact}}(x, y) &= (x + y) \cdot (1 + i) + \exp(x^2 + i y^2), \\ f(x, y) &= -((2x)^2 + (2i y)^2 + 2(1+i)) \cdot \exp(x^2 + i y^2) + k^2 \cdot u_{\text{exact}}(x, y), \\ g(x, y) &= (1+i) + (2i y) \cdot \exp(x^2 + i y^2) + i k \cdot u_{\text{exact}}(x, y). \end{aligned} \quad (18)$$

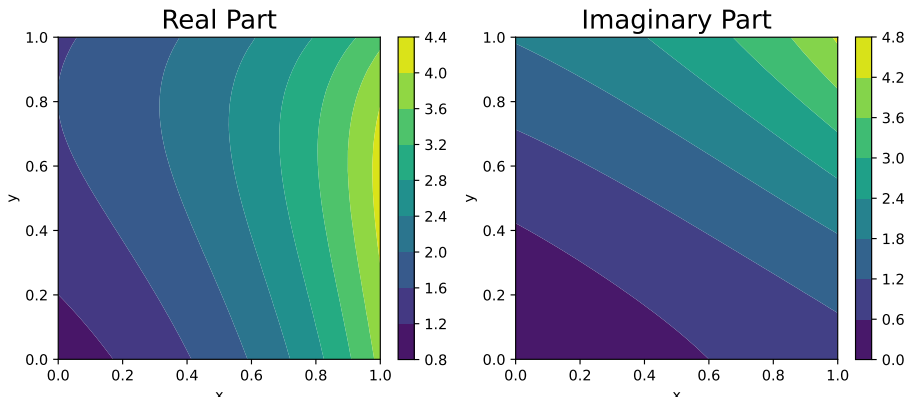


Figure 4: Real and Imaginary part of u_{exact} .

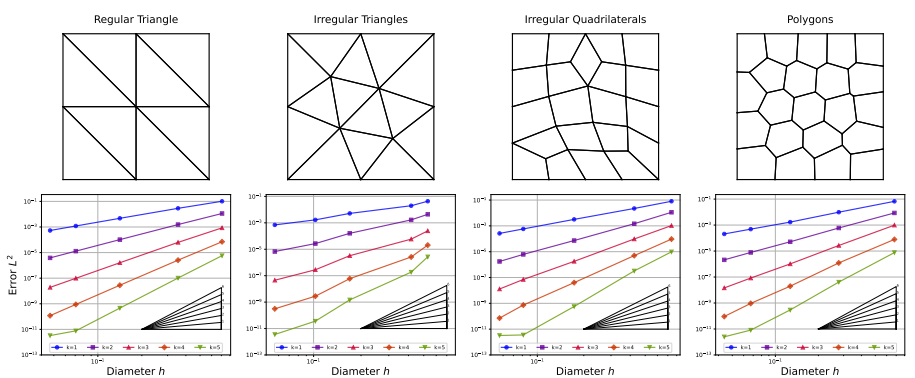
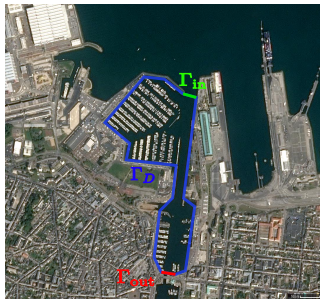
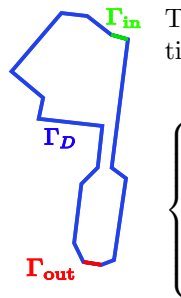


Figure 5: Convergence of order $\mathcal{O}(h^{k+1})$



Port location



Port boundary

The Helmholtz or **Mild-Slope** equation:

$$\left\{ \begin{array}{ll} \nabla(\mathbf{C}_p \mathbf{C}_g \nabla a) + k^2 \mathbf{C}_p \mathbf{C}_g a = 0, & \text{in } \Omega, \\ a = 0, & \text{in } \Gamma_{\text{in}}, \\ \frac{\partial a}{\partial n} + ik a = 0, & \text{in } \Gamma_{\text{out}}, \\ a = \gamma a_i & \text{in } \Gamma_{\mathbf{D}}. \end{array} \right.$$

5 Numerical Application

On prend un truc bidon sur un port ou qqc du genre

5.1 Sensibilité de la pente, helmoltz vs Berkhoff

On introduit un déferlement selon ([Munk 1949](#)) Problem conditions:

- $a_{\max} = 2 \text{ m},$
- $T_0 = 8 \text{ s},$
- $\theta = 280^\circ.$

5.2 Application claquée - Résultats avec différents k

Problem conditions:

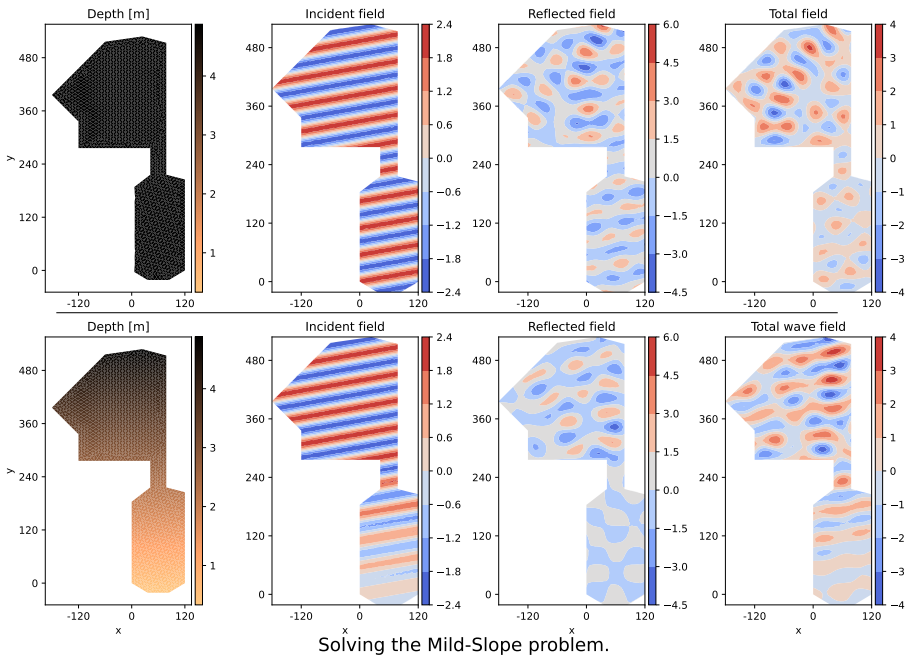
- $a_{\max} = 1 \text{ m},$
- $T_0 = 8 \text{ s},$
- $\theta = 250^\circ.$

5.3 Sensibilité du coefficient de réflexion

Problem conditions:

- $a_{\max} = 1 \text{ m},$
- $T_0 = 8 \text{ s},$
- $\theta = 280^\circ.$

Solving the Helmholtz problem.



Solving the Mild-Slope problem.

Figure 6: Caption

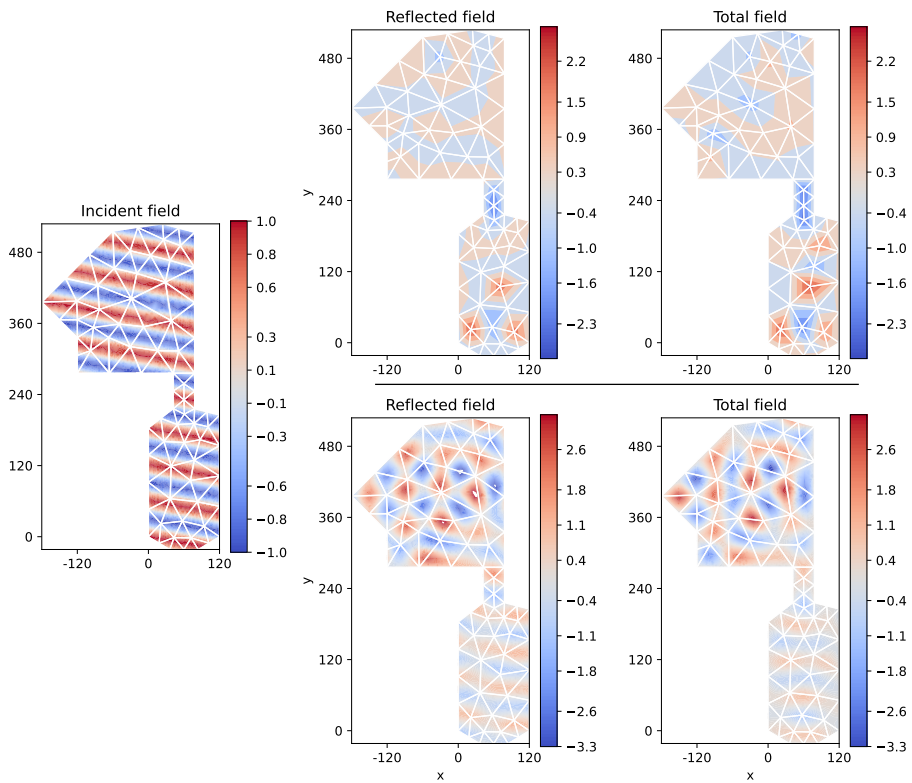
5.4 Appli montrant intérêt Robin

$$\begin{cases} \Delta u + k^2 u = 0 & , \quad \text{in } \Omega , \\ u = -u_{\text{inc}} & , \quad \text{on } \Gamma_D , \\ \frac{\partial u}{\partial n} + i k u = 0 & , \quad \text{on } \Gamma_{\text{Inf}} . \end{cases}$$

or

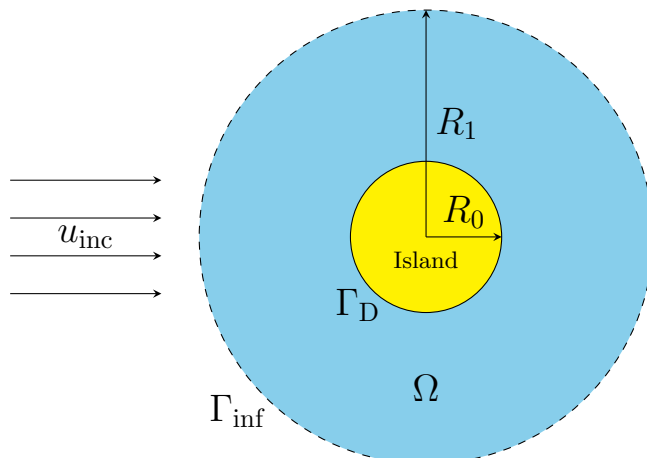
$$\begin{cases} \Delta u + k^2 u = 0 & , \quad \text{in } \Omega , \\ u = -u_{\text{inc}} & , \quad \text{on } \Gamma_D , \\ \frac{\partial u}{\partial n} = 0 & , \quad \text{on } \Gamma_{\text{Inf}} . \end{cases}$$

Solving the Helmholtz problem with $k=1$



Solving the Helmholtz problem with $k=5$

Figure 7: Caption



- $a_{\max} = 1 \text{ m}$,

Solving the Helmholtz problem with $\gamma = 1$

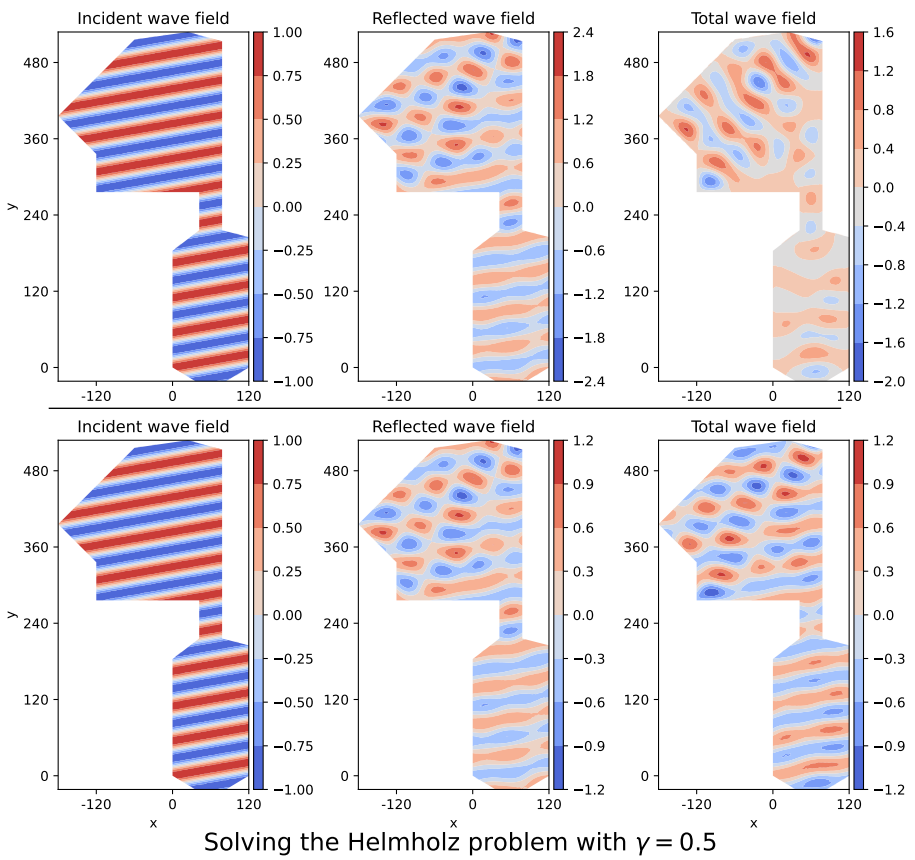


Figure 8: Caption

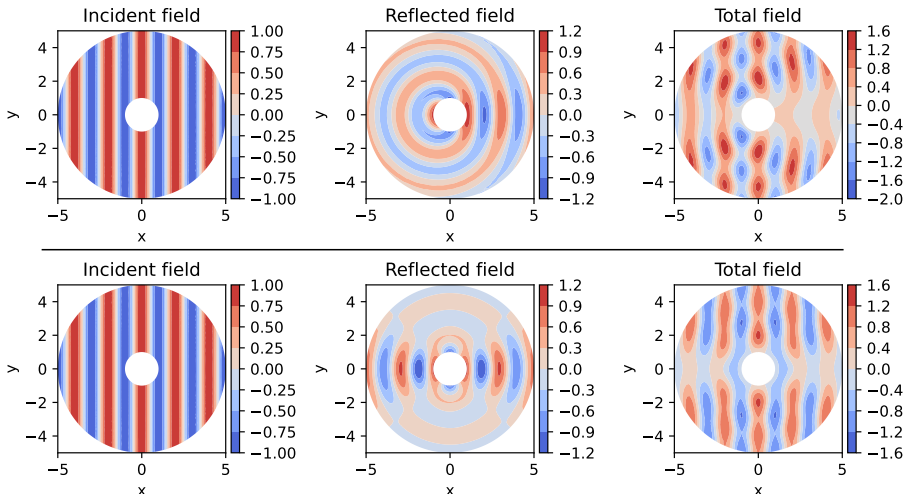
- $T_0 = 20$ s,

- $\theta = 0^\circ$.

6 Conclusion and Discussion

On est content

Solving the Helmholtz problem with a Robin condition on Γ_{inf}



Solving the Helmholtz problem with a Neuman condition on Γ_{inf}

Figure 9: Caption

7 Declarations

7.1 Availability of data and material

All data, models, and code generated or used during the study are available on request.

7.2 Conflict of interest

The authors declare that they have no conflict of interest.

7.3 Acknowledgements

This work was conducted as part as M. Dupont's PhD studies which is funded by the CNRS with the MITI grant. We gratefully acknowledge funding from CNRS, OPTIBEACH projects and FEDER Europe.

Appendix

A Roro pue

References

- Beirão da Veiga, L., F. Brezzi, L. D. Marini, and A. Russo (2014). “The Hitch-hiker’s Guide to the Virtual Element Method”. In: *Mathematical Models and Methods in Applied Sciences* 24.08, pp. 1541–1573. DOI: [10.1142/S021820251440003X](https://doi.org/10.1142/S021820251440003X).
- Berkhoff, J.C.W. (1972). “COMPUTATION OF COMBINED REFRACTION - DIFFRACTION”. In: *Coastal Engineering Proceedings* 1.13, p. 23. DOI: [10.9753/icce.v13.23](https://doi.org/10.9753/icce.v13.23).
- Booij, N. (1983). “A note on the accuracy of the mild-slope equation”. In: *Coastal Engineering* 7.3, pp. 191–203. DOI: [https://doi.org/10.1016/0378-3839\(83\)90017-0](https://doi.org/10.1016/0378-3839(83)90017-0).
- Helmholtz, Professor (1868). “XLIII. On discontinuous movements of fluids”. In: *The London, Edinburgh, and Dublin Philosophical Magazine and Journal of Science* 36.244, pp. 337–346.
- Mascotto, Lorenzo, Ilaria Perugia, and Alexander Pichler (2019). “A nonconforming Trefftz virtual element method for the Helmholtz problem”. In: *Mathematical Models and Methods in Applied Sciences* 29.09, pp. 1619–1656. DOI: [10.1142/S0218202519500301](https://doi.org/10.1142/S0218202519500301).
- Munk, Walter (1949). “The solitary wave theory and its application to surf problems”. In: *Annals of the New York Academy of Sciences* 51, pp. 376–424. DOI: [10.1111/j.1749-6632.1949.tb27281.x](https://doi.org/10.1111/j.1749-6632.1949.tb27281.x).
- Perugia, Ilaria, Paola Pietra, and Alessandro Russo (2016). “A plane wave virtual element method for the Helmholtz problem”. In: *ESAIM: Mathematical Modelling and Numerical Analysis* 50.3, pp. 783–808. DOI: [10.1051/m2an/2015066](https://doi.org/10.1051/m2an/2015066).